DESIGN, FABRICATION, AND CHARACTERIZATION OF SINGLE CRYSTAL SILICON LATCHING SNAP FASTENERS FOR MICRO ASSEMBLY

Rama Prasad
Sibley School of Mechanical
and Aerospace Engineering

Karl-Friedrich Böhringer
Robotics & Vision Laboratory
Department of Computer Science
Cornell University, Ithaca, NY 14853

Noel C. MacDonald
School of Electrical Engineering &
The National Nanofabrication Facility

ABSTRACT

A snap fastener is a deformable device consisting of a pair of mating surfaces that "snap" together during assembly. Because of the simple, linear assembly motion, such latching micro fasteners have a wide range of applications in micro assembly tasks, e.g. for devices with multiple or layered components, or micro opto-mechanical plugs. At the micro scale, conventional types of fasteners like screws and hinges are unlikely to work due to present fabrication constraints and large friction forces. Micro snap fasteners also have great potential to be used as sensors with memory.

We present a detailed theoretical analysis of design and function of micro snap fasteners, and describe the fabrication in single crystal silicon (SCS) technology. We perform experiments on snap fasteners with $1-2$ μm wide latches. Independent comb drive actuators generating micro-Newton forces were used for actuation of the fasteners to verify the theoretically obtained design rules. Our experimental results are in close accordance with the theoretical predictions.

1 INTRODUCTION

We have designed, analyzed, fabricated and characterized SCS micro snap fasteners. A standard SCREAM process (Zhang and MacDonald 1992, Shaw et al. 1993) was used to fabricate various designs of the fasteners. The stiffness of the snap fastener (i.e. the force required to engage the micro fastener latches) was tested using electrostatic micro comb actuators. We conducted a detailed mechanism analysis, from which we obtained rules for the design of micro snap fasteners.

Our devices have two outer latches and a central anchor (see Figure 1). The latches are supported on flexible cantilever beams. Using our actuator, successful

latching was observed with forces in the range of 30 μN, for beams of length 50 μm and width 2 μm. The total height of the beams fabricated with SCREAM was 8.5 μm. The latches are 1.5 μm wide, and their mating surfaces are angled at 45°. These design parameters can be varied over a wide range to change the stiffness of the fastener.
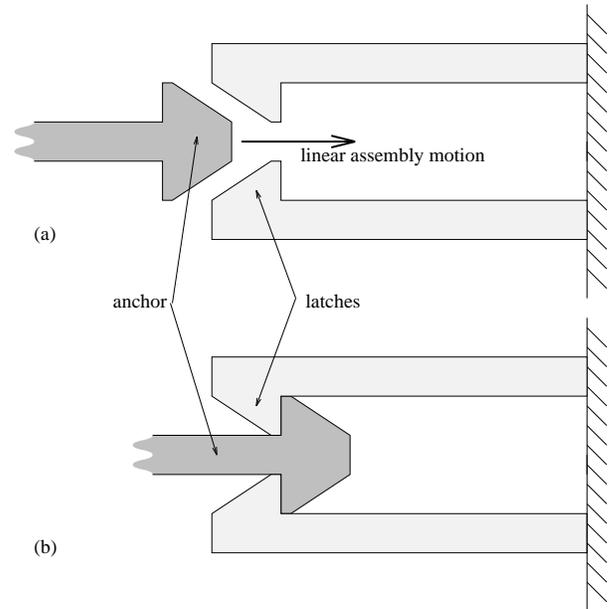
Figure 1: Functional principle of a snap fastener: (a) disengaged; (b) engaged.

Applications

Because of their simple design and functionality, snap fasteners are ideal devices for assembly in the micro

domain. Conventional types of fasteners like screws and nuts are less likely to work in micro assembly because of their complicated structure and motion with high friction. Different configurations of the basic latching mechanism can be used for a wide range of applications for micro sensors, in micro assembly and micro robotics.

Vertical micromechanical velcro has been built and characterized by Han et al. (1992). These structures have arrays of SiO_2 caps on silicon pedestals and have been used for wafer bonding. Pressure exceeding 12 kPa is required to bond the velcro surfaces together. The disengaging strength of the bond is larger than 240 kPa.

Ciarlo (1992) uses latching silicon structures as accelerometers for moderate and high-g applications. They consist of two cantilever beams that interlock at a set threshold acceleration which is determined by their design.

Polysilicon structures with integrally fabricated hinges have been designed by Pister et al. (1992). The hinges rotate out of plane and get fixed in a vertical position by a locking mechanism which is similar to snap fasteners. The hinges interconnect with other structures to form 3D devices like micro-probes, parallel plate grippers, or Fresnel lens arrays.

Micro Assembly.   Complicated micro structures consisting of multiple components can be assembled together in the plane using snap fasteners. They also have great potential when being lifted out of plane and used as vertical plug-in connectors. Multi-layered structures can be built using these plugs. Currently under investigation is another application for micro opto-mechanical plugs, in which optical fibers are accurately attached. The connectors can be used both for electrical or insulated connections.

Sensors with Memory.   These fasteners have tremendous applications as sensors. Varying configurations in combination with supporting electronic circuitry can be used to sense pressure, temperature, acceleration, impact etc. They can be designed to measure either force or displacement. Their hysteretic behaviour allows them to be used as sensors with memory. Arrays of these devices with increasing stiffness can be used to determine the magnitude of the engaging force.

Overview

In the following section we give a detailed description of snap fastener design and mechanism analysis. We identify the design parameters and describe their effect in terms of design rules. Section 3 contains the fabrication process and its effect on the mechanism design. In Section 4 we present the results from our experiments and compare them with our theoretical predictions. Sec-

tion 5 summarizes our work and gives an outlook on future work and open questions.

2 DESIGN AND MECHANICAL ANALYSIS

A snap fastener consists of a mating pair of an *anchor* and flexible *latches* (see Figure 1). In its disengaged state anchor and latches can move freely with respect to each other. To engage the device, the anchor is moved along a straight line towards the latches as depicted in Figure 1(a), such that the anchor comes in sliding contact with the latches, causing them to bend outward, until the anchor is fully inside the latches. The following properties of snap fasteners are of particular interest:

1. Assembly is simpler than e.g. with screws or nuts, as only a linear motion is required to engage the components.
2. Assembly is robust, i.e. small errors in the relative position of anchor and latches are corrected automatically by their chamfered surfaces.
3. The force required to engage the fastener can be chosen over a wide range depending on the shape and size of the device.
4. The force to engage can be made much smaller than the force to disengage (*motion diode*).
5. The device has two stable states, *disengaged* and *engaged*, with hysteresis characteristics depending on the device design.

Snap fastener design and analysis follow the discussion by Donald and Pai (1991), where a more detailed theoretical analysis can be found.
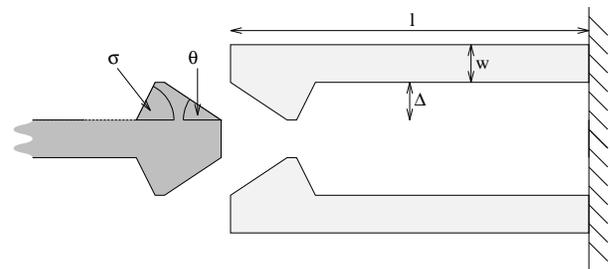
Figure 2: Design schematic of a snap fastener.

Mechanism Design

Consider the schematic drawing of a snap fastener in Figure 2. Each latch consists of a flexible cantilever beam of length l, width w, and (not shown) height h. At the tip of the beam there is a latching mechanism whose shape matches with the anchor. The anchor has chamfered sides, such that the front chamfer is sloped at an angle θ, and the back chamfer is sloped at an angle

σ. The width of overlap between latch and anchor is called Δ.

(a)

(b)
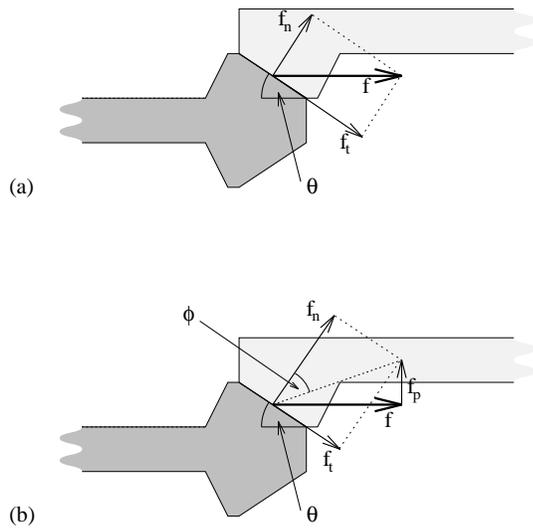
Figure 3: Forces during snap fastener assembly: (a) sticking contact (higher coefficient of friction), (b) sliding contact (lower coefficient of friction).

Mechanism Analysis

In the following we analyze the design in greater detail. Assume we want to engage the snap fastener by applying a force f in the direction of assembly. Once anchor and latch are in contact, there are two possibilities: anchor and latch are in sticking frictional contact (Figure 3(a)), or in sliding frictional contact (Figure 3(b)). For sticking contact, f will cause a normal force $f_n = f \sin \theta$ acting on the latch. The tangential component $f_t = f \cos \theta$ will be balanced out by the friction force f_r.

Previous work by Prasad et al. (1995) has shown that we can assume Coulomb friction, where the friction force f_r is proportional to the normal force f_n and the friction coefficient μ, such that $f_r = \mu f_n$. Under Coulomb friction sticking occurs when the tangential force f_t is less than the friction force f_r. To avoid sticking we must therefore make sure that the following condition holds:

$$f_t > f_r$$
$$\text{so} \quad f \cos \theta > \mu f \sin \theta$$
$$\text{which implies} \quad \cot \theta > \mu \quad (1)$$

A similar analysis applies for disassembly, where θ will be replaced by σ.

If the device is in sliding frictional contact, Coulomb's friction law predicts that normal force f_n

and (tangential) friction force $f_r = f_t$ are related by $f_t = \mu f_n$. It follows that the angle ϕ in Figure 3(b) is independent of the applied force f, and $\tan \phi = f_t / f_n = \mu$. Therefore, the sum $f_n + f_t$ is in general not equal to the applied force f. The difference is a perpendicular force f_p which has to be provided by the anchor structure. This perpendicular force will push the latch outward until it engages.
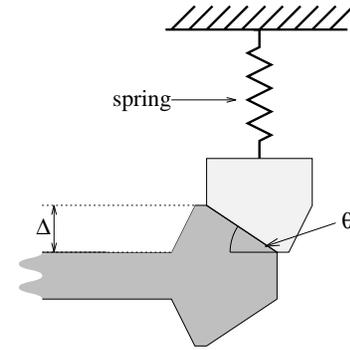
Figure 4: Linear spring model for snap fastener.

For the small angles of deflection occuring during assembly we can model the latches as linear springs obeying the relationship $f_\delta = K \delta$, with spring constant K, deflection δ, and corresponding retracting force f_δ (see Figure 4). The spring constant can be determined from the latch geometry by $K = \frac{3EI}{l^3}$, where E is the Young's Modulus, and $I = \frac{hw^3}{12}$ (for derivation of formulas see e.g. Juvinall and Marshek (1983)).

To overcome the spring force f_δ we get the following condition:

$$f_p > f_\delta \quad \text{for all } \delta$$
$$\text{so} \quad f \cot(\phi + \theta) > f_\Delta$$
$$\text{which implies} \quad f > K \Delta \tan(\phi + \theta)$$
$$= K \Delta \frac{\mu + \tan \theta}{1 - \mu \tan \theta} \quad (2)$$

Equations (1) and (2) specify the design rules for snap fasteners. They state that $\cot \theta$ has to be greater than the friction coefficient μ. They further predict that the force necessary to engage a snap fastener is proportional to the spring constant $K = \frac{3EI}{l^3}$, the latch overlap Δ, and the tangent of $\phi + \theta$.

Design Parameters

We define stiffness of a snap fastener as the force required to engage a particular fastener configuration. The design parameters affecting the stiffness of the fasteners are the length l, width w and height h of the supporting beams (Figure 2). The latch overlap Δ and the angle θ also effect the stiffness according to equation (2). The width w and height h are constrained by
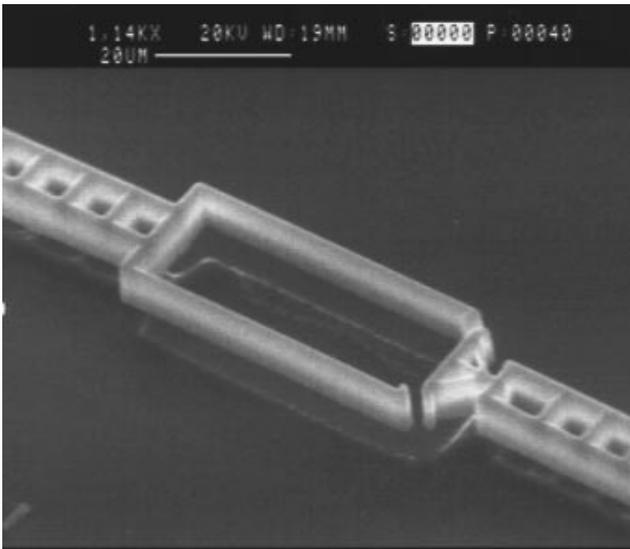
Figure 5: Micro snap fastener (SEM micrograph).

Figure 6: Micro snap fastener (detail).
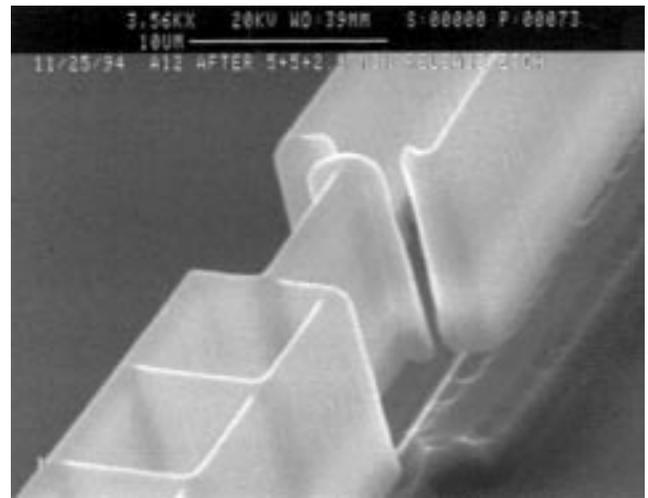
Figure 7: Micro snap fastener (side view).

the SCREAM process. To ensure release using standard SCREAM the final beams cannot be wider than 2 μm, and for straight side walls obtainable from Cl_2 RIE we have restricted the height to at most 10 μm. The width of the latches has been chosen to be 1 μm such that the total width of the beam and the latches is not larger than 2 μm for release. The angle θ has been selected to be 45°. The coefficient of friction for SCREAM fabricated surfaces has been determined by Prasad et al. (1995) to range from 0.3 to 0.5. Figures 5 – 7 show SEM pictures of such devices.

We have chosen the length l of the beams and the chamfer angle θ to be the design parameters of major interest, as they can be varied over a wide range of values, and they have the maximum effect on the stiffness. We have built fasteners with lengths ranging from 20 μm to 50 μm. However, very long cantilevered beams (> 100 μm) may sag and bend out of plane due to residual stresses arising from processing.

Actuator Device

To test the stiffness of the snap fasteners, we have mounted them on lateral comb drive actuators. These actuators have been well characterized by Prasad et al. (1995). Two actuators exert the engaging force from both sides of the fastener (Figure 8). Each actuator has $N = 350$ fingers on ladder beams. The final gap between fingers after fabrication is $d = 1.5$ μm, and the height of the fingers is $h = 8.5$ μm. The force generated by these actuators is given (Prasad et al. 1995) by the formula

$$ f \;=\; \frac{1}{2}\,\epsilon\,h\,N\,V^2\,/\,d \qquad (3) $$

which for our values is $f = 1.32 \times 10^{-8}$ (V^2) N, for a voltage V in volts. We can apply up to 80 V across the fingers without break down of the passivating oxide layer. This generates forces up to 80 μN, which is well within the range of the force required to engage the snap fasteners for the beam lengths we have studied.

Design Automation

There exist efficient computational tools for analysis and simulation of snap fasteners. Donald and Pai (1991) have presented an efficient algorithm to automatically analyze snap fasteners with arbitrary designs, and predict their behavior during compliant frictional contact. Using their techniques it is possible to automatically generate the appropriate design of a snap
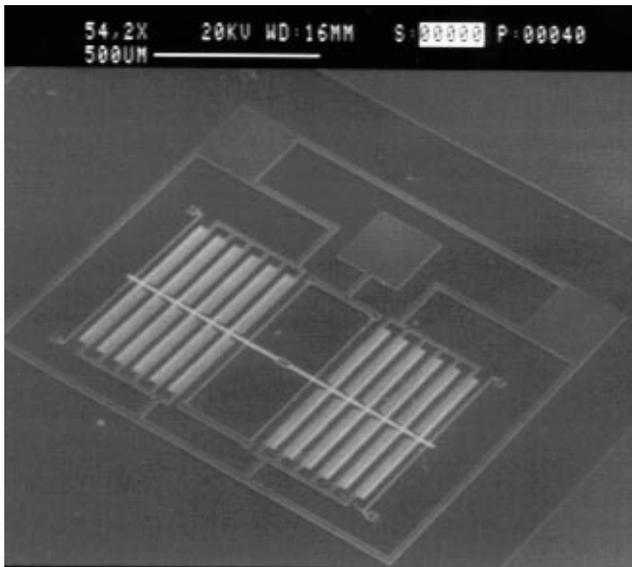
Figure 8: Micro comb drive actuator (SEM micrograph).

fastener given just the functional specification of the device. An outline for such an automatic design algorithm has been presented by Böhringer (1993). Combined with the highly automated VLSI fabrication process, this allows a virtually completely automated production, making snap fasteners one of the very few devices that can be fabricated automatically given only their functional specification.

3 DEVICE FABRICATION

We have used standard SCREAM to fabricate our device. The layout of the complete device comprising of the fastener latches and the two actuators was drawn using SYMBAD, a CAD package for IC circuits. SCREAM (Zhang and MacDonald 1992, Shaw et al. 1993) is a single mask, reactive ion etching process for the fabrication of submicron, movable single-crystal silicon electromechanical structures. We followed a variation of SCREAM for releasing 2 μm wide beams.

The process flow for releasing a beam in cross section is shown in Figure 9. PECVD is used to deposit insulating layers of SiO$_2$. Chlorine based reactive ion etching is used for trench etching into the silicon substrate. On the starting substrate of arsenic-doped, 0.005 Ωcm, n-type (100) silicon wafer, a 2.4 μm thick etch mask layer of silicon dioxide was deposited using plasma enhanced chemical vapor deposition at 300° C, 450 mT, N$_2$O flow of 42 sccm and SiH$_4$ flow of 12 sccm for 60 min. Photolithography is used to transfer the pattern from the mask onto a layer of KTI 985i 16.5cs positive

Step 1: Prepare Mask Oxide
← Mask Oxide (1-2µm)
← Silicon Substrate (SCS)

Step 2: Photolithography
← Exposed Photoresist
← Mask Oxide
← Silicon Substrate (SCS)

Step 3: Transfer Pattern
← Exposed Photoresist
← Mask Oxide
← Silicon Substrate (SCS)

Step 4: Strip Resist
← Mask Oxide
← Silicon Substrate (SCS)

Step 5: Deep Silicon Etch
← Mask Oxide
← Silicon Substrate (SCS)

Step 6: Deposit Sidewall Oxide
← PECVD Sidewall oxide (0.3µm)
← Mask Oxide
← Silicon Substrate (SCS)

Step 7: Remove Floor Oxide
← Mask Oxide
← Silicon Substrate (SCS)

Step 8: Deep Silicon Etch #2
← Mask Oxide
← Silicon Substrate (SCS)

Step 9: Release Etch
← Mask Oxide
← Silicon Substrate (SCS)

Step 10: Sputter Metallization
← Sputtered Metal (Al)
← Mask Oxide
← Silicon Substrate (SCS)

Figure 9: SCREAM process flow.

resist spun on the oxide. The minimum feature size in our device is 1 μm thick beams of our fastener. The pattern is transferred from the resist layer to the oxide layer using MRC Magnetron ion etching at 2 mT at a flow rate of 30 sccm of CHF_3 at 1000 W. The photo resist is removed using O_2 plasma etch.

The pattern is transferred into the silicon substrate from the silicon oxide layer using Cl_2 reactive ion etching in a Plasma Therm PK-1250 at 30 mT, 450 V and at a flow rate of 50 sccm for Cl_2 and 1.5 sccm BCl_3 for 45 min to get 8 μm deep trenches. This trench depth determines the beam heights. We used lower pressure and higher voltage for nearly vertical sidewalls. The sidewall slopes determine contact area when the fastener is latching. Vertical side walls are desirable as flared side walls will lead to line contact at the bottom of the latches leading to unpredictable behavior. Following this an insulating layer of silicon dioxide is deposited for side wall passivation using PECVD at the parameter values stated above for 15 min giving a 400 nm thick oxide layer. CHF_3 reactive ion etching is again used to remove the floor oxide for subsequent substrate etches.

A short Cl_2 reactive ion etch at 50 sccm Cl_2 and 5 sccm BCl_3, 40 mT and 400 V for 20 min generates 5 μm deep trenches in the substrate to aid in the following release etch of 2 μm wide beams. All the beams of thickness up to 2 μm are released from the silicon substrate using SF_6 RIE process in a Plasma Therm 72 RIE system. A SF_6 plasma with a SF_6 flow rate of 140 sccm at 90 mT and 150 W was used to release the beams in 6 min. A 100 nm thin layer of silicon oxide was deposited to avoid any shorting between the conducting Al layer and the silicon substrate. A 500 nm layer of Al is conformally deposited using DC magnetron sputtering performed at 30 mT pressure, with a beam current of 5 A and argon flow rate of 30 sccm.

A 100 nm thick layer of oxide is finally deposited on the device to avoid shorting when the latches make contact during operation. The structural beams finally are 8.5 μm tall, including the deposited layers. The cantilever beams comprising the latches are 50 μm long, 8.5 μm tall and are finally 2.0 μm thick.

Design Modifications

For our initial design we had used latch dimensions of $l = 50$ μm, $w = 1$ μm, $\Delta = 1.5$ μm, and $\theta = 45°$ (Figure 2). The gap between the two outer latches was 10 μm. This gap was too small, so that the PECVD oxide did not coat the inner and outer side walls uniformly, leading to residual stressed which bend the beams outward. To ensure uniform films on both inner and outer walls we changed the fastener design to more widely spaced beams ranging from 20 μm to 40 μm. Another variation was to put two beams on the outside of the inner beams, leading to both side walls of the latch beams
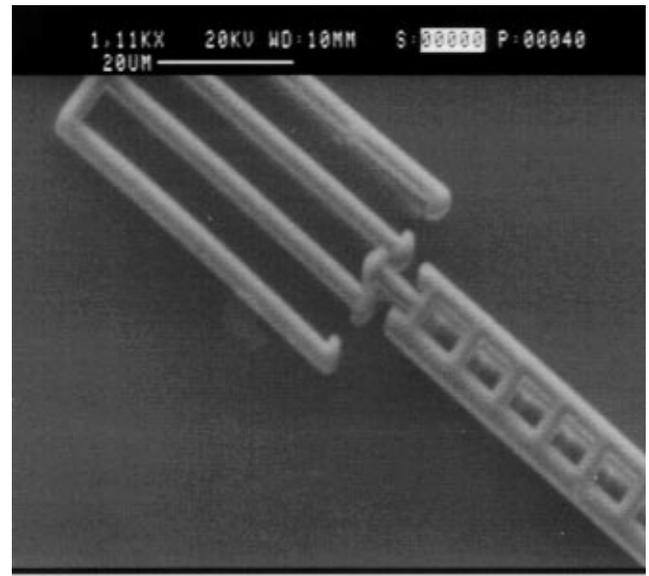
Figure 10: Engaged micro snap fastener (SEM micrograph).

being 10 μm away from other beam sidewalls (Figures 5 and 10). Both variations produce straight cantilevered beams for supporting the latches using the standard SCREAM process outlined above.

4 EXPERIMENTAL RESULTS AND PERFORMANCE

Predictions from Design Analysis

We now use the theoretical results from Section 2 to predict the behavior of our micro snap fasteners. From Equation (2) we know that the force f required to engage a snap fastener is

$$f = K \ \Delta \ \tan(\phi + \theta) = \frac{3(EI)_{\text{eff}}}{l^3} \ \Delta \ \tan(\phi + \theta)$$

The SCREAM fabrication process gives us beams coated with films of SiO_2 of 0.5 μm thickness. The silicon core is 1 μm wide and 8 μm high. Hence, the effective spring constant K_{eff} is composed of K_{Si} of the Si beam core, and K_{SiO_2} of the coating.

$$
\begin{aligned}
K_{Si} &= \frac{190 \text{ GPa } 8 \text{ } \mu\text{m } (1 \text{ } \mu\text{m})^3}{4 \text{ } (50 \text{ } \mu\text{m})^3} \\
&= 3.04 \text{ N/m} \\
K_{SiO_2} &= [73 \text{ GPa } (8 \text{ } \mu\text{m } ((2 \text{ } \mu\text{m})^3 - (1 \text{ } \mu\text{m})^3) \\
&\quad + 0.5 \text{ } \mu\text{m } (2 \text{ } \mu\text{m})^3)] \text{ / } (4 \text{ } (50 \text{ } \mu\text{m})^3) \\
&= 8.76 \text{ N/m}
\end{aligned}
$$

$K_{\text{eff}} = K_{Si} + K_{SiO_2} = 11.8$ N/m (K_{Al} for the thin Al layer is neglectable). E is the Young's Modulus. Figure 11 shows the relationship between beam length
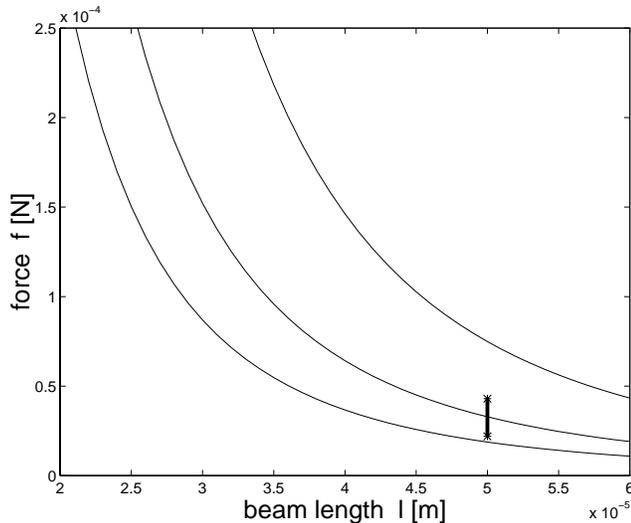
Figure 11: Relationship between chamfer beam length l and assembly force f for chamfer angles (top to bottom) $\theta = 60°$, $45°$, and $30°$.

l and required force f for three different chamfer angles. Δ was 1.5 μm, and $\mu = 0.3$.

Experimental Results

We observed engagement of our snap fasteners with the design as described above at voltages between 50 and 70 V. According to Equation (3) in Section 2 this implies forces in a range between 22 and 43 μN. This range is drawn in Figure 11 as vertical bar. We observe that theoretical predictions match with the experimental results.

5 CONCLUSIONS AND FUTURE WORK

We have described a SCS micro snap fastener. From the mechanism analysis presented, we can vary the stiffness of such fasteners, using the design rules developed above as guidelines. SCREAM was used to fabricate the device consisting of the fasteners and the actuators generating the force required for engagement. Some design modifications were incorporated to get closely spaced parallel beams 1 μm wide and 50 μm long using SCREAM. The fasteners were successfully engaged using the actuators at the predicted voltage of 50 V, generating 30 μN, which verifies our analysis.

The design rules can be used to construct different variations of these fasteners. Other configurations allowing us capabilities like controlled disengagement can also be similarly built using the latches and actuators with SCREAM. We also propose to investigate the effect of the various design parameters, as well as study of wear on repeated snap operations.

Snap fasteners have a wide range of applications, especially for various sensors with memory, for the assembly of complex micro devices, for micro opto-mechanical structures, and in micro robotics.

REFERENCES

Böhringer, Karl-Friedrich 1993. A computational approach to the design of micromechanical hinged structures. In *Proceedings of the ACM/SIGGRAPH Symposium on Solid Modeling and Applications*, Montréal, Québec, Canada. ACM Press.

Ciarlo, Dino R. 1992. A latching accelerometer fabricated by the anisotropic etching of (110) oriented silicon wafers. *Journal of Micromechanics and Microengineering* 2.

Donald, Bruce R. and Pai, Dinesh K. 1991. The motion of compliantly connected rigid bodies in contact. *Int. Journal of Robotics Research*.

Han; Weiss; and Reed 1992. Micromechanical velcro. *Journal of Microelectromechanical Systems*.

Juvinall, Robert C. and Marshek, Kurt M. 1983. *Fundamentals of Machine Component Design*. Wiley, New York.

Pister, K.S.J.; Judy, M.W.; Burgett, S.R.; and Fearing, R.S. 1992. Microfabricated hinges. *SAA* 33(3):249–256.

Prasad, Rama; MacDonald, Noel C.; and Taylor, Dean 1995. Micro-instrumentation for tribological measurements. In *Transducers — Digest Int. Conf. on Solid-State Sensors and Actuators*, Stockholm, Sweden.

Shaw, Kevin A.; Zhang, Z. Lisa; and MacDonald, Noel C. 1993. SCREAM I: A single mask, single-crystal silicon process for microelectromechanical structures. In *Transducers — Digest Int. Conf. on Solid-State Sensors and Actuators*, Pacifico, Yokohama, Japan.

Zhang, Z. Lisa and MacDonald, Noel C. 1992. An RIE process for submicron, silicon electromechanical structures. *Journal of Micromechanics and Microengineering* 2(1):31–38.